Synergistic Induction of Oxidative Injury and Apoptosis in Human Multiple Myeloma Cells by the Proteasome Inhibitor Bortezomib and Histone Deacetylase Inhibitors

Xin-Yan Pei,[1] Yun Dai,[1] and Steven Grant[1,2,3]

Departments of [1]Medicine, [2]Biochemistry, and [3]Pharmacology, Virginia Commonwealth University, Medical College of Virginia, Richmond, Virginia

ABSTRACT

Purpose: The purpose of this study was to examine interactions between the proteasome inhibitor bortezomib (Velcade) and the histone deacetylase (HDAC) inhibitors sodium butyrate and suberoylanilide hydroxamic acid in human multiple myeloma (MM) cells that are sensitive and resistant to conventional agents.

Experimental Design: MM cells were exposed to bortezomib for 6 h before the addition of HDAC inhibitors (total, 26 h), after which reactive oxygen species (ROS), mitochondrial dysfunction, signaling and cell cycle pathways, and apoptosis were monitored. The functional role of ROS generation was assessed using the free radical scavenger *N*-acetyl-ʟ-cysteine.

Results: Preincubation with a subtoxic concentration of bortezomib markedly sensitized U266 and MM.1S cells to sodium butyrate- and suberoylanilide hydroxamic acid-induced mitochondrial dysfunction; caspase 9, 8, and 3 activation; and poly(ADP-ribose) polymerase degradation; resulting in synergistic apoptosis induction. These events were associated with nuclear factor κB inactivation, c-Jun NH$_2$-terminal kinase activation, p53 induction, and caspase-dependent cleavage of p21^{CIP1}, p27^{KIP1}, and Bcl-2, as well as Mcl-1, X-linked inhibitor of apoptosis, and cyclin D1 downregulation. The bortezomib/HDAC inhibitor regimen markedly induced ROS generation; moreover, apoptosis and c-Jun NH$_2$-terminal kinase activation were attenuated by *N*-acetyl-ʟ-cysteine. Dexamethasone- or doxorubicin-resistant MM cells failed to exhibit cross-resistance to the bortezomib/HDAC inhibitor regimen, nor did exogenous interleukin 6 or insulin-like growth factor I block apoptosis induced by this drug combination. Finally, bortezomib/ HDAC inhibitors induced pronounced lethality in primary CD138$^+$ bone marrow cells from MM patients, but not in the CD138$^-$ cell population.

Conclusions: Sequential exposure to bortezomib in conjunction with clinically relevant HDAC inhibitors potently induces mitochondrial dysfunction and apoptosis in human MM cells through a ROS-dependent mechanism, suggesting that a strategy combining these agents warrants further investigation in MM.

INTRODUCTION

Multiple myeloma (MM) is an incurable hematological disorder characterized by the dysregulated proliferation of terminally differentiated plasma cells. Until relatively recently, the mainstays of treatment for MM, aside from bone marrow transplantation, consisted of cytotoxic drugs (*e.g.,* melphalan, vincristine, and doxorubicin) and steroids [*e.g.,* dexamethasone (1)]. Over the last several years, significant insights into the pathogenesis of MM have emerged, including the contribution to myeloma cell survival made by growth factors [*e.g.,* interleukin (IL)-6 and insulin-like growth factor (IGF)-I (2, 3)], stromal cells (4), and dysregulation of various signal transduction pathways, including those related to nuclear factor (NF)-κB, Akt, and extracellular signal-regulating kinase 1/2, among others (3, 5, 6). These insights have prompted the search for new compounds that specifically target pathways on which myeloma cells depend for their survival. Such efforts have culminated in the introduction of several new agents into the therapeutic armamentarium for MM, including thalidomide (7), arsenic trioxide (8), and, most recently, proteasome inhibitors (9).

Proteasome inhibitors represent a diverse group of agents that target the 20S proteasome, a component of the ubiquitin-proteasome complex that is responsible for the degradation of unwanted cellular proteins (10). Although the mechanism by which proteasome inhibitors kill neoplastic cells is not known with certainty, sparing of proapoptotic proteins such as Bax and p53 has been proposed (11, 12). Alternatively, proteasome inhibition leads to cytoplasmic accumulation of the IκBα protein, which binds to the NF-κB transcription factor, preventing it from translocating to the nucleus, where it triggers transcription of various antiapoptotic genes (10). Bortezomib (Velcade) is a boronic acid inhibitor of the catalytic site of the 20S proteasome that has recently entered clinical trials in humans (9, 13). In preclinical studies, bortezomib has been shown to be a potent inducer of apoptosis in human MM cells (14), a finding that may reflect the critical importance of NF-κB signaling in myeloma cell survival (11). Importantly, clinical trials in humans have demonstrated that bortezomib is highly active in MM, including

that which occurs in patients who have become refractory to standard forms of therapy (9, 15).

Histone deacetylase (HDAC) inhibitors are compounds that inhibit HDACs, enzymes that, in conjunction with histone acetylases, regulate the acetylation state of histones and, by extension, the conformational status of chromatin (16). In general, HDAC inhibitors, by promoting histone acetylation, permit chromatin to assume a more relaxed state, thereby allowing transcription of genes involved in various cellular processes, including differentiation, particularly in malignant hematopoietic cells (17). However, when administered at higher concentrations, HDAC inhibitors induce apoptosis, a phenomenon that has been related to induction of oxidative injury (18, 19). Two such compounds are the short chain fatty acid sodium butyrate [NaB (20)] and suberoylanilide hydroxamic acid (SAHA), an agent that is currently undergoing clinical evaluation in patients with hematological malignancies (21). Recently, preclinical studies indicate that SAHA exhibits significant activity against MM cells *in vitro* (22), raising the possibility that HDAC inhibitors may have a role to play in myeloma treatment.

In an earlier study, coadministration of HDAC inhibitors with the proteasome inhibitor MG-132 was shown to induce a marked increase in mitochondrial injury and apoptosis in Y79 retinoblastoma cells (23). More recently, we have reported that bortezomib interacts synergistically with HDAC inhibitors to induce apoptosis in Bcr/Abl$^+$ as well as Bcr/Abl$^-$ acute leukemia cell types (24). Because of the established efficacy of bortezomib in MM (14, 15) and preliminary evidence of the preclinical activity of HDAC inhibitors in this disease (22), it would clearly be desirable to determine whether similar interaction might occur in myeloma cells. To address this issue, we have examined interactions between bortezomib and several HDAC inhibitors (*e.g.,* NaB and SAHA) in MM cell lines that are sensitive and resistant to established cytotoxic agents. Here we report that combined exposure of myeloma cells to bortezomib and HDAC inhibitors results in a synergistic increase in mitochondrial injury, caspase activation, and apoptosis in association with multiple perturbations in signal transduction pathways and through an antioxidant-sensitive but IL-6- and IGF-I-insensitive process. Moreover, similar synergistic interactions occur in MM cells that are highly resistant to cytotoxic drugs such as doxorubicin as well as dexamethasone. Together, these findings suggest that a therapeutic strategy combining bortezomib and clinically relevant HDAC inhibitors warrants further examination in MM and related hematological malignancies.

MATERIALS AND METHODS

Cells and Reagents. The human MM cell lines U266 and RPMI8226 were purchased from American Type Culture Collection (Manassas, VA). The dexamethasone-sensitive (MM.1S) and dexamethasone-resistant (MM.1R) human MM cell lines were kindly provided by Dr Steven T. Rosen (Northwestern University, Chicago, IL; Ref. 25). Cells were maintained in RPMI 1640 containing 10% fetal bovine serum, 200 units/ml penicillin, 200 μg/ml streptomycin, minimal essential vitamins, sodium pyruvate, and glutamine. Doxorubicin-resistant sublines (Dox40) of RPMI8226 cells were kindly provided by Dr Wil-

liam S. Dalton (University of South Florida, Tampa, FL; Ref. 26) and maintained in RPMI 1640 as described above containing 400 nM doxorubicin.

The specific proteasome inhibitor bortezomib (Velcade; formerly known as PS-341) was kindly provided by Millennium Pharmaceuticals Inc. (Cambridge, MA). The HDAC inhibitors SAHA and NaB were purchased from Calbiochem (San Diego, CA). These agents were dissolved in DMSO as a stock solution, stored at −80°C, and subsequently diluted with serum-free RPMI 1640 before use. *N*-Acetyl-L-cysteine (L-NAC; Calbiochem) was prepared in sterile water immediately before use. Dexamethasone (Sigma, St. Louis, MO) was dissolved in DMSO, aliquoted, and stored at −20°C. Recombinant human IL-6 and IGF-I were purchased from Sigma and R&D Systems (Minneapolis, MN) and rehydrated in PBS and 10 mM acetic acid (both of which contained 0.1% BSA, respectively), aliquoted, and stored at −80°C. Caspase inhibitor t-butyloxycarbonyl-Asp(Ome)-fluoromethyl ketone (BOC-D-fmk) was provided by Enzyme System Products (Livermore, CA), dissolved in DMSO, and stored at 4°C. In all experiments, the final concentration of DMSO did not exceed 0.1%.

Experimental Format. All experiments were performed using logarithmically growing cells ($4-6 \times 10^5$ cells/ml). Cell suspensions were placed in sterile Falcon tissue culture dishes (Becton Dickinson, Franklin Lakes, NJ) and pretreated with bortezomib for 6 h at 37°C. At the end of this period, either SAHA or NaB was added to the suspension without washing the cells free of bortezomib, and the dishes were placed in a 37°C, 5% CO_2 incubator for various intervals (generally 20 h). In some studies, cells were pretreated with L-NAC for 3 h before bortezomib. BOC-fmk, IL-6, or IGF-I was added concurrently with bortezomib. Alternatively, in some experiments, cells were simultaneously exposed to these agents (*e.g.,* for 26 h) or to the reverse sequence (*e.g.,* SAHA for 6 h, followed by the addition of bortezomib for 20 h). After drug treatment, cells were harvested and subjected to further analysis as described below.

Assessment of Apoptosis. The extent of apoptosis was evaluated by assessing Wright-Giemsa-stained cytospin slides under light microscopy and scoring the number of cells exhibiting classic morphological features of apoptosis. For each condition, 5–10 randomly selected fields/slide were evaluated, encompassing at least 800 cells. To confirm the results of morphological analysis, in some cases apoptosis was also evaluated by annexin V-FITC staining and flow cytometry, and cell viability was determined by trypan blue exclusion. Briefly, 1×10^6 cells were stained with annexin V-FITC (BD PharMingen, San Diego, CA) and 5 μg/ml propidium iodide in 1× binding buffer [10 mM HEPES/NaOH (pH 7.4), 140 mM NaOH, and 2.5 mM $CaCl_2$] for 15 min at room temperature in the dark. The samples were analyzed by flow cytometry within 1 h to determine the percentage of cells displaying annexin V$^+$ (early apoptosis) or annexin V$^+$/propidium iodide$^+$ staining (late apoptosis). In all cases, results of morphological analysis correlated highly with results of annexin V/propidium iodide staining ($r > 0.90$).

Cell Survival Assays. For cell viability assays, MTS (MTS, 3(4,5-dimethylthiazol-2-yl)-5-(3-carboxymethoxyphenyl)-2-(4-sulfophenyl)-2H-tetrazolium, inner salt), CellTiter 96 AQueous One Solution (Promega, Madison, WI) was used as

per the manufacturer's instructions, and the absorbance at 490 nm was recorded using a 96-well plate reader (Molecular Devices, Sunnyvale, CA; Ref. 27).

Analysis of Mitochondrial Membrane Potential ($\Delta\Psi_m$). Cells (2×10^5) were stained with 40 nM 3,3-dihexyloxacarbocyanine (Molecular Probes, Eugene, OR) in PBS at 37°C for 20 min and then analyzed by flow cytometry. The percentage of cells exhibiting a decreased level of 3,3-dihexyloxacarbocyanine uptake, which reflects loss of $\Delta\Psi_m$, was determined using Becton-Dickinson FACScan (Becton-Dickinson, San Jose, CA).

Western Blot Analysis. Western blot samples were prepared from whole-cell pellets as described previously (28). The amount of total protein was quantified using Coomassie Protein Assay Reagent (Pierce, Rockford, IL). Equal amounts of protein (30 μg) were separated by SDS-PAGE and electrotransferred onto nitrocellulose membrane. For analysis of protein phosphorylation, sodium vanadanate and Na PP$_i$ (1 mM each) were added to 1× sample buffer, no SDS was included in the transfer buffer, and TBS was used instead of PBS throughout. The blots were probed with the appropriate dilution of primary antibody as follows. Where indicated, the blots were reprobed with actin antibody (BD PharMingen) or tubulin antibody (Transduction Laboratories, San Diego, CA) to ensure equal loading and transfer of proteins. The primary antibodies included the following: phospho-p44/42 mitogen-activated protein kinase (extracellular signal-regulating kinase, Thr^{202}/Tyr^{204}) antibody (Cell Signaling, Beverly, MA); phospho-c-Jun NH$_2$-terminal kinase [JNK (Thr^{183}/Tyr^{185})] antibody (Santa Cruz Biotechnology, Santa Cruz, CA); stress-activated protein kinase/JNK antibody (Cell Signaling); phospho-p38 mitogen-activated protein kinase (Thr^{180}/Tyr^{182}) antibody (Santa Cruz Biotechnology); anti-p21$^{CIP/WAF1}$ (Transduction Laboratories); anti-p27^{KIP1} (BD PharMingen); p53 antibody (Santa Cruz Biotechnology); antihuman Bcl-2 oncoprotein (Dako, Carpinteria, CA); Bcl-x$_{S/L}$ antibody (S-18; Santa Cruz Biotechnology); X-linked inhibitor of apoptosis (XIAP) antibody (Cell Signaling); Mcl-1 antibody (BD PharMingen); cyclin D1 antibody (BD PharMingen); poly-(ADP-ribose) polymerase (PARP) antibody (Biomol, Plymouth Meeting, PA); anti-caspase 8 (Alexis); anti-caspase 9 (BD PharMingen); anti-caspase 3 (Transduction Laboratories), cleaved caspase 3 antibody (Cell Signaling); and anti-acetyl-histone H3 and H4 (Upstate Biotechnology, Lake Placid, NY).

Analysis of Cytosolic Cytochrome *c* and Smac/DIABLO. Cells (4×10^6) were lysed by incubating them in lysis buffer (75 mM NaCl, 8 mM Na$_2$HPO$_4$, 1 mM NaH$_2$PO$_4$, 1 mM EDTA, and 350 μg/ml digitonin). The lysates were centrifuged at $12,000 \times g$ for 1 min, and the supernatant, consisting of the cytosolic S-100 fraction, was collected in an equal volume of 2× sample buffer. The proteins were quantified, separated by 15% SDS-PAGE, and subjected to Western blot as described above. Cytochrome *c* antibody (BD PharMingen) and Smac/DIABLO antibody (Upstate Biotechnology) were used as primary antibodies.

Measurement of Cellular Reactive Oxygen Species (ROS) Production. Dichlorodihydroflurescein, which is nonfluorescent in the dihydro-dichlorodihydroflurescein form but becomes highly fluorescent on reaction with ROS, was used to monitor production of cellular ROS (29). Briefly, 2×10^5 cells were incubated with 10 μM aceto-oxymethyl ester of dihydro-dichlorodihydroflurescein (Molecular Probes) in PBS at 37°C for 30 min and then analyzed by flow cytometry. The production of ROS was determined by comparing increased intensity of dichlorodihydroflurescein for drug-treated *versus* untreated control cells.

Electrophoretic Mobility Shift Assay. Nuclear extracts were prepared as described previously (30). Double-stranded oligonucleotides corresponding to the NF-κB binding site of immunoglobulin κ promoter were obtained from Promega and labeled with [γ-^{32}P]ATP (3000 Ci/mmol; ICN Biomedicals, Irvine, CA) using T4 polynucleotide kinase (Promega) and purified using a MicroSpin G-25 column (Amersham Pharmacia, Piscataway, NJ). Nuclear extracts (5 μg) were incubated at 4°C for 20 min with 10^5 cpm of labeled oligonucleotide probe in binding buffer [20 mM HEPES (pH 7.9), 5 mM MgCl$_2$, 4 mM DTT, 20% glycerol, 0.1 mM phenylmethylsulfonyl fluoride, 5 mM benzamidine, 2 mM levamisol, 0.1 μg/ml aprotinin, 0.1 μg/ml bestatin, and 2 μg poly(deoxyinosinic-deoxycytidylic acid)]. The reaction mixtures were electrophoresed in 6% native polyacrylamide gels in 0.5× Tris-borate EDTA (pH 8.0), and the gels were dried at 80°C and exposed to X-ray film for autoradiography.

Isolation of CD138$^+$ Myeloma Cells. Bone marrow samples were obtained with informed consent from two patients with MM undergoing routine diagnostic aspirations. Approval was obtained from the institutional review board of Virginia Commonwealth University for these studies. Informed consent was provided according to the Declaration of Helsinki. CD138$^+$ and CD138$^-$ cells were separated using an MS$^+$/LS$^+$ column and a magnetic separator according to the manufacturer's instructions (Miltenyi Biotec; Ref. 27). The purity of CD138$^+$ cells (>90%) was monitored by CD138-phycoerythrin staining and flow cytometry. Viability of the cells was regularly >95% by trypan blue exclusion. CD138$^+$ and CD138$^-$ cells were cultured in RPMI 1640 containing 10% FCS in 96-well plates under the same condition described above. After drug treatment, the percentage of apoptotic cells was evaluated by examining Wright-Giemsa-stained cytospin preparations under light microscopy.

Statistical Analysis. For morphological assessment of apoptotic cells, annexin V analysis, analysis of $\Delta\Psi_m$, analysis of ROS production, and cell survival assays, experiments were repeated at least three times. Values represent the means ± SD for at least three separate experiments performed in triplicate. The significance of differences between experimental variables was determined using Student's *t* test. Analysis of synergism was performed according to median dose-effect analysis (31) using a commercially available software program (Calcusyn; Biosoft, Ferguson, MO).

RESULTS

Bortezomib Interacts Synergistically with SAHA and NaB to Induce Mitochondrial Injury in U266 Myeloma Cells. To determine what effect combined exposure to bortezomib and HDAC inhibitors would have on myeloma cell survival, U266 cells were preincubated with 2.4 nM bortezomib for 6 h, after which either 1 μM SAHA or 1 mM NaB was added for an additional 20 h. As shown in Fig. 1*A*, bortezomib, SAHA,
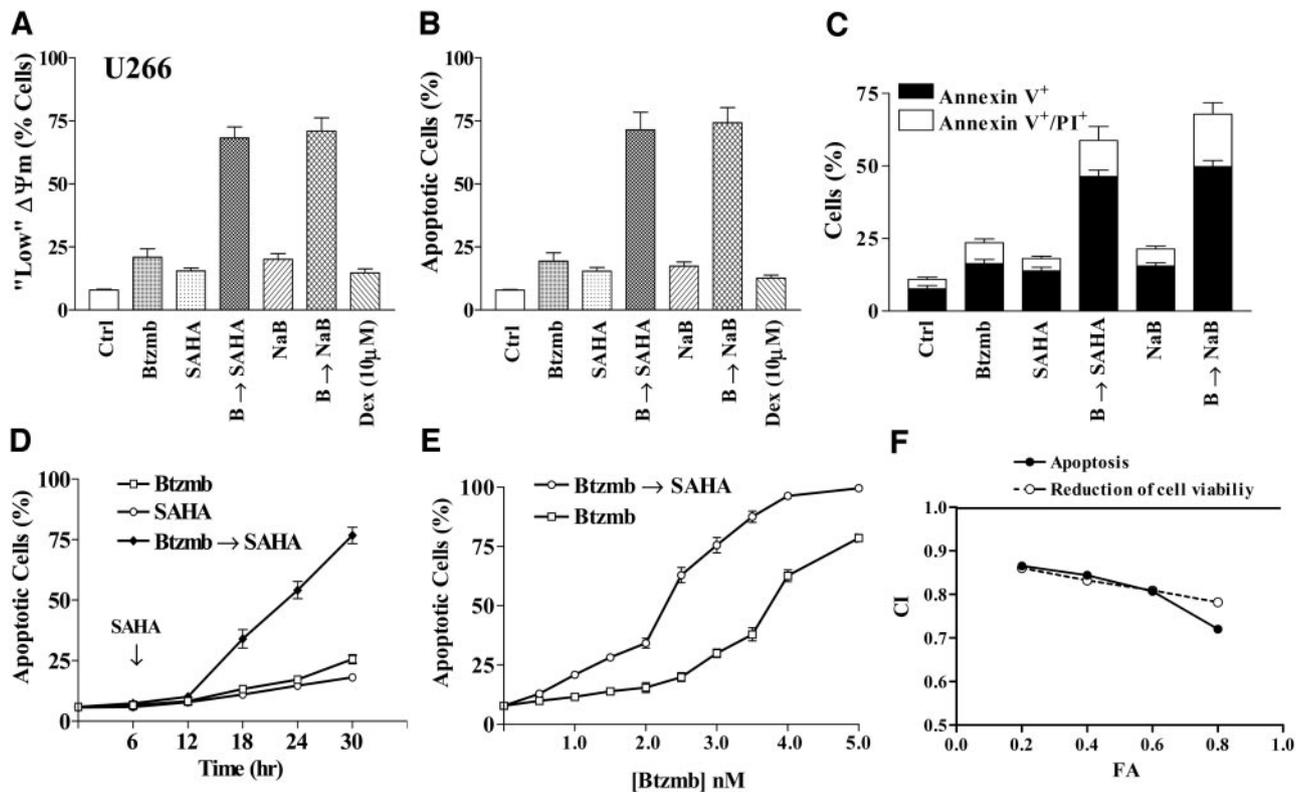
Fig. 1 Pretreatment with bortezomib synergistically potentiates apoptosis induced by histone deacetylase inhibitors in multiple myeloma cells. U266 cells were treated sequentially with 2.4 nM bortezomib (*Btzmb*; 6 h) followed, without washing, by 1 μM suberoylanilide hydroxamic acid (SAHA) or 1 mM sodium butyrate for 20 h, after which the percentage of cells exhibiting loss of $\Delta\Psi m$ (*A*) and apoptotic morphology (*B*) was determined by flow cytometric analysis of 3,3-dihexyloxacarbocyanine staining and evaluation of Wright Giemsa-stained cytospin preparations as described in "Materials and Methods." For comparison, cells were exposed to 10 μM dexamethasone for 24 h. Alternatively, U266 cells were treated as described above, after which the percentage of apoptotic cells was monitored by annexin V-FITC staining and flow cytometry. Annexin V$^+$/propidium iodide$^-$ corresponds to early apoptosis, and annexin V$^+$/propidium iodide$^+$ corresponds to late apoptosis (*C*). U266 cells were treated with SAHA after 6 h of pretreatment with bortezomib. At the indicated intervals, the percentage of cells exhibiting apoptotic morphology was determined as described above (*D*). U266 cells were exposed to 1 μM SAHA for 20 h, after b-h preincubation with the indicated concentration (in nM) of bortezomib, after which the percentage of cells exhibiting apoptotic morphology was determined by evaluation of Wright Giemsa-stained cytospin preparations (*E*). For *A*–*E*, values represent the means ± SD for three separate experiments performed in triplicate. U266 cells were exposed to a range of bortezomib and SAHA concentrations alone and in combination at fixed ratio (*e.g.*, 1:400) in a sequential manner (bortezomib, 6 h → SAHA, 20 h). At the end of this period, the percentage of cells exhibiting apoptotic morphology was determined for each condition (*F*). Median dose-effect analysis was used as described in "Materials and Methods" to characterize the nature of the interaction between SAHA and bortezomib administered at a fixed ratio of 400:1. End points were apoptosis (morphology; ●) or trypan blue dye exclusion (○). For each fraction affected, a combination index value was calculated. Combination index values < 1.0 correspond to a synergistic interaction. Two additional studies yielded equivalent results.

or NaB administered alone only modestly reduced mitochondrial membrane potential ($\Delta\Psi_m$) compared with controls (*e.g.*, 10–15%), whereas combined exposure led to a reduction in ~75% of cells. By comparison, exposure of cells to a high concentration of dexamethasone (10 μM) for the same interval resulted in minimal apoptosis (*e.g.*, <15%). Comparable results were obtained when apoptosis was monitored by cell morphology (Fig. 1*B*) or by annexin V/propidium iodide staining (Fig. 1*C*). In separate studies, greater-than-additive effects were also observed when cells were simultaneously exposed to bortezomib and HDAC inhibitors for 26 h (*e.g.*, without bortezomib preincubation) or exposed to the sequence HDAC inhibitor for 6 h followed by addition of bortezomib for 20 h, but these effects were not as pronounced as those obtained in cells preincubated with bortezomib. For example, in U266 cells, values for simultaneous administration were as follows: SAHA (1.0

μM) alone, 15.6 ± 5.1% apoptotic cells; bortezomib (2.4 nM), 19.4 ± 6.1% apoptotic cells; and the combination, 47.4 ± 5.7% apoptotic cells. For the sequence SAHA followed by bortezomib, values were 15.5 ± 2.7% apoptotic cells (SAHA), 13.5 ± 4.1% apoptotic cells (bortezomib), and 37.3 ± 3.7% apoptotic cells for the combination (data not shown). No schedule resulted in antagonistic effects. Consequently, for all subsequent studies, the optimal schedule involving 6-h pretreatment with bortezomib before addition of HDAC inhibitors was used.

Time course studies revealed that cells exposed to the combination of bortezomib and HDAC inhibitors exhibited a significant increase in apoptosis after 12 h of HDAC inhibitor treatment, which increased further over the ensuing 12 h (Fig. 1*D*). A bortezomib dose-response study revealed that addition of a subtoxic concentration of SAHA (1.0 μM) significantly increased bortezomib lethality over a range of concentrations,

Fig. 2 The bortezomib/histone deacetylase inhibitor regimen effectively induces apoptosis in drug-sensitive and -resistant multiple myeloma (MM) cells. Dexamethasone-sensitive (MM.1S; *A*) and -resistant (MM.1R; *C*) MM cells were sequentially treated for 6 h with bortezomib (MM.1S, 2.2 nM; MM.1R, 2 nM) followed by suberoylanilide hydroxamic acid (1 μM) or sodium butyrate (MM.1S, 1 mM; MM.1R, 0.5 mM) for 20 h, after which the percentage of cells exhibiting apoptotic morphology was determined by evaluating Wright Giemsa-stained cytospin preparations. For comparison, cells were exposed to 10 μM dexamethasone for 24 h. Alternatively, MM.1S (*B*) and MM.1R (*D*) cells were treated as described above, after which the MTS assay was used to monitor cell survival and proliferation. RPMI8226 MM cells (*E*) and their doxorubicin-resistant counterparts (Dox40; *F*) were incubated for 6 h with 6 nM bortezomib followed by treatment for 20 h with 1.5 μM suberoylanilide hydroxamic acid, after which the percentage of cells exhibiting apoptotic morphology was determined as described above. Results represent the means ± SD for three separate experiments performed in triplicate.
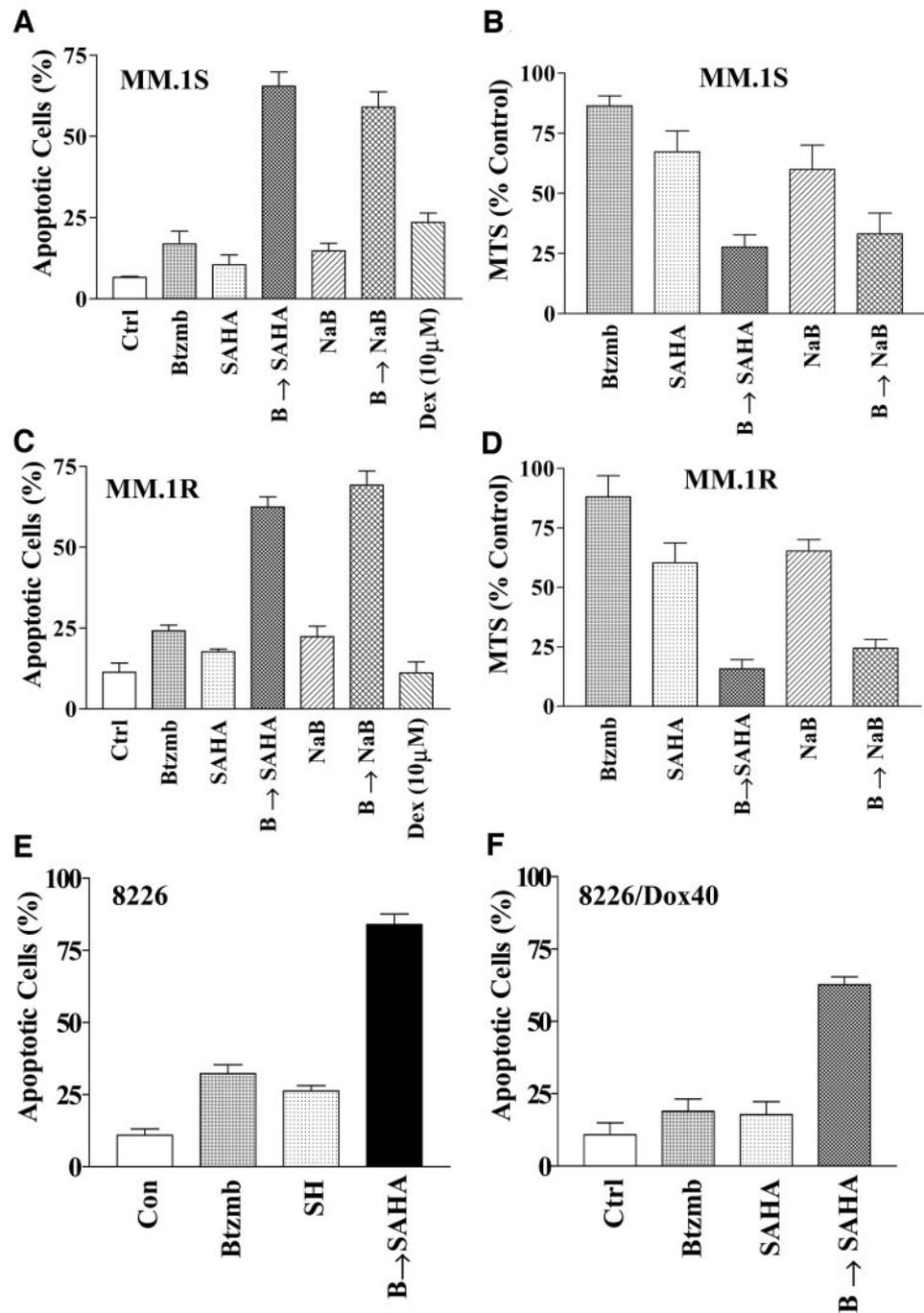
including those (*e.g.,* 0.5–2.5 nM) that were nontoxic by themselves (Fig. 1*E*). In separate studies, administration of SAHA by itself at concentrations as high as 5.0 μM was only modestly toxic to these cells (*e.g.,* < 20% apoptosis; data not shown). Finally, median dose-effect analysis (using either apoptosis or reduction of cell viability by trypan blue exclusion as an end point) in U266 cells exposed to bortezomib and SAHA at a fixed ratio (1:400) yielded combination index values of <1.0, corresponding to a synergistic interaction (Fig. 1*F*).

Bortezomib and HDAC Inhibitors Effectively Trigger Apoptosis in Drug-Sensitive and -Resistant Myeloma Cell Lines. Attempts were made to extend the preceding findings to other myeloma cell lines. Individual treatment of MM.1S cells with bortezomib (2.3 nM), SAHA (1 μM) or NaB (1 mM) only modestly induced apoptosis or diminished survival (as determined by MTS assays), whereas sequential exposure to bortezomib followed by SAHA or NaB resulted in a major increase in cell death, reflected by an increase in apoptosis and
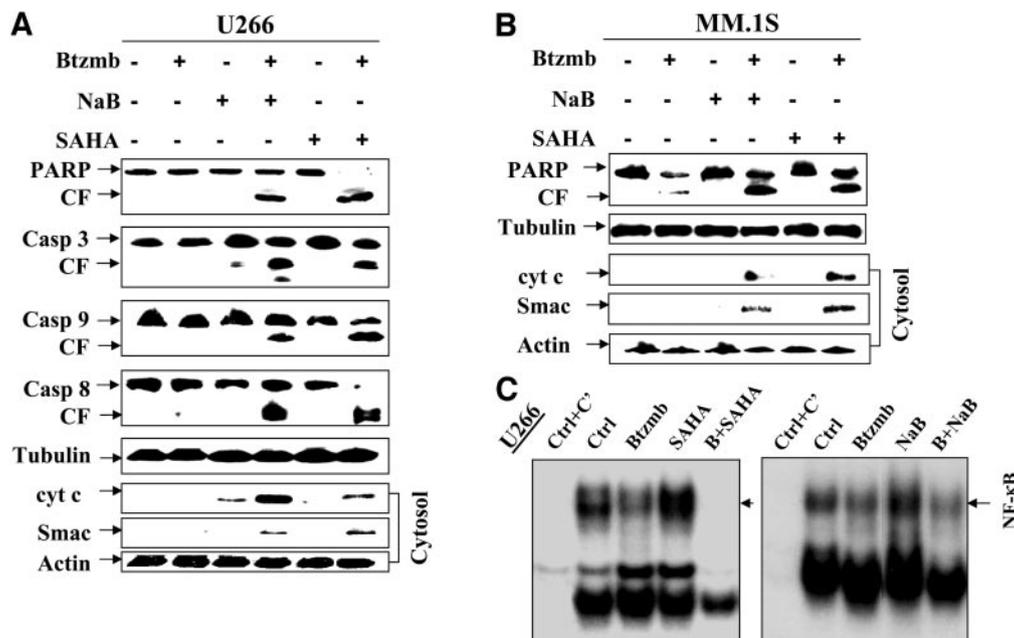
Fig. 3 The bortezomib/histone deacetylase inhibitor regimen induces apoptosis through activation of the mitochondrial pathway and caspase cascade, accompanied by inhibition of constitutive nuclear factor (NF)-κB activity in multiple myeloma (MM) cells. *A,* after a 6-h preincubation with 2.4 nM bortezomib, U266 cells were treated with 1 μM suberoylanilide hydroxamic acid or 1 mM sodium butyrate for 20 h. At the end of this period, the cells were lysed and subjected to Western blot analysis using the indicated primary antibodies. *CF,* cleavage fragment. Alternatively, cytosolic (S-100) fractions were obtained as described in "Materials and Methods," and expression of cytochrome *c* and Smac/DIABLO was monitored by Western blot. (*B*) MM.1S cells were pretreated with 2.3 nM bortezomib for 6 h followed by exposure to 1 μM suberoylanilide hydroxamic acid or 1 mM sodium butyrate for 20 h. Western blot analysis was performed to monitor degradation of poly(ADP-ribose) polymerase and cytosolic expression of cytochrome *c* and Smac/DIABLO as described above. For *A* and *B,* each lane was loaded with 30 μg of protein; blots were stripped and reprobed with antiactin or antitubulin antibodies to ensure equal loading and transfer of protein. Two additional studies yielded equivalent results. *C,* U266 cells were treated as described above, after which nuclear extracts were prepared and subjected to electrophoretic mobility shift assay as described in "Materials and Methods." The activity of NF-κB was reflected by the extent of binding of ^{32}P-labeled oligonucleotides corresponding to the NF-κB binding site of the immunoglobulin κ promoter. To control for probe specificity, nuclear extracts obtained from untreated cells were incubated with a 100-fold excess of unlabeled NF-κB oligonucleotides for 10 min before the addition of labeled NF-κB oligonucleotides (*Lane 1; Ctrl+C'*). The results of a representative experiment are shown; two additional studies yielded equivalent results.

loss of viability by MTS assay (Fig. 2, *A* and *B*). By comparison, 10 μM dexamethasone was only modestly toxic to these cells (*e.g.,* ∼20% apoptosis; Fig. 2*A*). Furthermore, essentially identical results were obtained in dexamethasone-resistant MM.1R cells (Fig. 2, *C* and *D*), indicating that the mechanisms conferring steroid resistance to this myeloma cell line failed to protect cells from the bortezomib/HDAC inhibitor regimen. MM.1R cells were essentially immune to the lethal effects of 10 μM dexamethasone. Similarly, sequential treatment with bortezomib and SAHA resulted in a pronounced (and equivalent) increase in apoptosis in doxorubicin-sensitive and -resistant RPMI8226 cells (Fig. 2, *E* and *F*). It should be noted that a higher concentration of bortezomib (*e.g.,* 6 nM) was used in studies involving Dox40 cells, which may reflect the multidrug resistance phenomenon. Nevertheless, a clear potentiation of SAHA lethality was observed in these cells as well. These findings indicate that combined exposure to bortezomib and either SAHA or NaB potently induces apoptosis in various myeloma cell lines, including those resistant to dexamethasone or doxorubicin.

Sequential Exposure of Myeloma Cells to Bortezomib and HDAC Inhibitors Potently Triggers Release of Proapoptotic Mitochondrial Proteins and Caspase Activation. To document that combined proteasome/HDAC inhibition did in

fact trigger classical apoptosis, Western analysis was used. As shown in Fig. 3*A*, treatment of U266 myeloma cells with bortezomib, SAHA, or NaB alone minimally triggered cleavage/ activation of caspase 9, 8, and 3; PARP degradation; or release of cytochrome *c* or Smac/DIABLO into the cytosolic S-100 fraction. In marked contrast, sequential exposure of cells to bortezomib followed by SAHA or NaB led to a clear increase in caspase activation, PARP cleavage, and cytosolic release of cytochrome *c* and Smac/DIABLO. Similar results were obtained in MM.1S cells (Fig. 3*B*). These findings indicate that combined treatment of myeloma cells with bortezomib and HDAC inhibitors potently induces caspase activation and release of proapoptotic mitochondrial proteins, events associated with activation of the apoptotic program.

MM Cells Exposed to Bortezomib and HDAC Inhibitors Exhibit a Reduction in NF-κB DNA Binding Activity. Electrophoretic mobility shift analysis was used to determine what effect combined exposure to bortezomib and HDAC inhibitors would have on NF-κB DNA binding activity in U266 cells (Fig. 3*C*). As anticipated, bortezomib treatment (2.4 nM) resulted in diminished NF-κB activity, whereas exposure to NaB or SAHA resulted in a modest increase in DNA binding. However, combined treatment was associated with a marked

Fig. 4 The bortezomib/histone deacetylase inhibitor regimen results in phosphorylation of stress-activated protein kinase/c-Jun NH$_2$-terminal kinase and induction of p53 in multiple myeloma (MM) cells. MM cells were incubated for 20 h with 1 μM suberoylanilide hydroxamic acid or 1 mM sodium butyrate after a 6-h pretreatment with bortezomib (*left panels,* U266, 2.4 nM; *right panels,* MM.1S, 2.3 nM), after which the cells were lysed and subjected to Western blot analysis using the indicated primary antibodies. *CF,* cleavage fragment. Each lane was loaded with 30 μg of protein; the blots were stripped and reprobed with antiactin antibody to ensure equal loading and transfer of protein. Two additional studies yielded equivalent results.
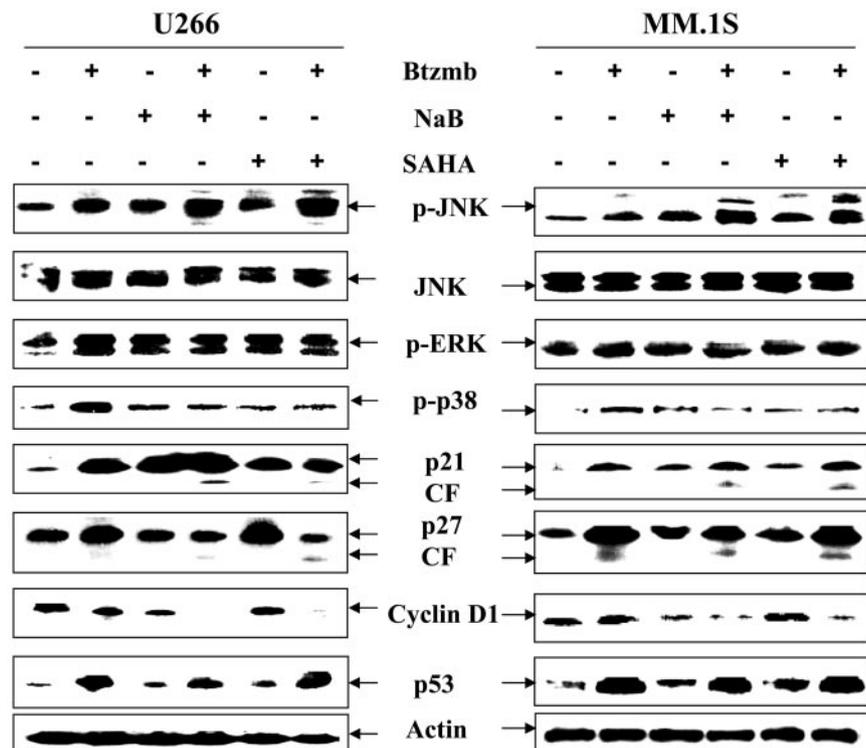
reduction in (NaB) or abrogation (SAHA) of NF-κB DNA binding activity. These findings raise the possibility that interactions between bortezomib and SAHA or NaB may reflect inactivation of the cytoprotective NF-κB signaling pathway.

Sequential Exposure of Myeloma Cells to Bortezomib and HDAC Inhibitors Results in Activation of JNK, Down-Regulation of Cyclin D1, and Induction of p53. The effects of combining bortezomib and SAHA or NaB on the expression/activation of various signaling molecules were then examined in U266 and MM.1S myeloma cells. As shown in the *left panels* of Fig. 4, exposure of U266 cells to bortezomib or HDAC inhibitors individually resulted in an increase in JNK phosphorylation but no changes in total JNK levels. Combined exposure led to a further increase in JNK activation. In contrast, no changes in extracellular signal-regulating kinase activation were noted. Bortezomib alone triggered an increase in p38 mitogen-activated protein kinase phosphorylation, but this effect was diminished by coadministration of HDAC inhibitors. Treatment of cells with bortezomib resulted in an increase in expression of the cyclin-dependent kinase inhibitors p21[CIP1] and p27[KIP1], whereas coadministration of HDAC inhibitors modestly induced cleavage of these proteins. Combined exposure of U266 cells to bortezomib and HDAC inhibitors was also associated with a pronounced down-regulation of cyclin D1. Finally, exposure of cells to bortezomib, with or without HDAC inhibitors, increased p53 expression. In each case, similar findings were obtained in MM.1S cells (Fig. 4, *right panels*). Thus, combined treatment of MM cells with bortezomib and HDAC inhibitors resulted in enhanced activation of the stress-related kinase JNK, cleavage of p21[CIP1] and p27[KIP1], down-regulation of cyclin D1, and induction of p53.

Combined Exposure of Myeloma Cells to Bortezomib and HDAC Inhibitors Is Associated with Bcl-2 Cleavage and Down-Regulation of Mcl-1 and XIAP. As shown in Fig. 5, coadministration of bortezomib did not appreciably change SAHA- or NaB-mediated acetylation of histones H3 and H4 in either U266 (*left panels*) or MM.1S cells (*right panels*). Although total levels of the Bcl-2 protein remained relatively constant, the appearance of a Bcl-2 cleavage product, which has been associated with proapoptotic actions (32), could be faintly detected in cells exposed sequentially to bortezomib and HDAC inhibitors. Exposure of myeloma cells to HDAC inhibitors, particularly the combination of HDAC inhibitors and bortezomib, resulted in down-regulation of inhibitor of apoptosis XIAP and survival factor Mcl-1 in both cell lines. Bcl-x$_L$ levels were modestly increased in bortezomib-exposed cells, but not in cells treated with both agents. Thus, sequential treatment of myeloma cells with bortezomib and HDAC inhibitors resulted in several perturbations in Bcl-2 family members that might plausibly contribute to the marked increase in apoptosis.

Bortezomib/HDAC Inhibitor-Mediated Lethality and Modulation of JNK Activation and Down-Regulation of Cyclin D1, Mcl-1, and XIAP Depend on Generation of ROS. Previous studies have suggested that the lethal effects of proteasome inhibitors administered alone in lung cancer cells (33) or in combination with HDAC inhibitors in Bcr/Abl$^+$ myeloid leukemia cells (24) stem from the generation of ROS. Studies were therefore performed to determine whether a similar mechanism might underlie bortezomib/HDAC inhibitor lethality in MM cells. As shown in Fig. 6A, sequential exposure of U266 cells to bortezomib and either NaB or SAHA was associated with a marked increase in ROS generation. Furthermore, coad-
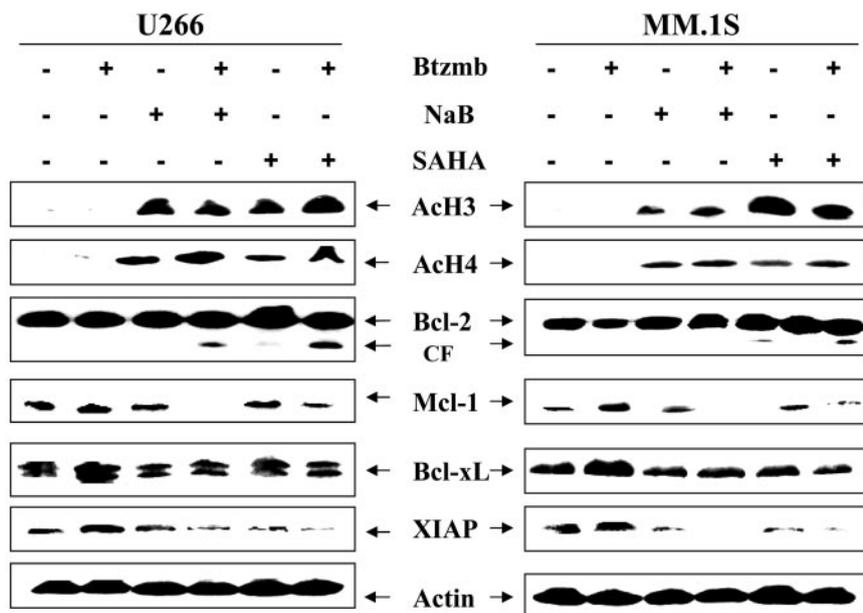
Fig. 5 The bortezomib/histone deacetylase inhibitor regimen induces multiple perturbations in expression of antiapoptotic proteins. After a 6-h preincubation with bortezomib (*left panels,* U266, 2.4 nM; *right panels,* MM.1S, 2.3 nM), multiple myeloma cells were treated with 1 μM suberoylanilide hydroxamic acid or 1 mM sodium butyrate for 20 h. At the end of this period, acetylation of histone H3 and H4 and expression of antiapoptotic proteins (*e.g.,* Bcl-2, Bcl-x_L, X-linked inhibitor of apoptosis, and Mcl-1) were monitored by Western blot. *CF,* cleavage fragment. Each lane was loaded with 30 μg of protein; the blots were stripped and reprobed with antiactin antibody to ensure equal loading and transfer. Results are representative of three separate experiments.

ministration of the antioxidant L-NAC (15 mM) substantially blocked bortezomib/HDAC inhibitor-mediated increases in ROS levels. Similar results were obtained in MM.1S cells (data not shown). Moreover, L-NAC also largely blocked bortezomib/HDAC inhibitor-mediated release of cytochrome *c* and Smac/DIABLO into the cytosolic S-100 fraction of U266 and MM1.S cells (Fig. 6*B*). Consistent with these findings, L-NAC significantly ($P < 0.01$) blocked bortezomib/HDAC inhibitor-mediated apoptosis in U266 and MM.1S cells (Fig. 6, *C* and *D*). Collectively, these findings indicate that generation of ROS plays a significant functional role in bortezomib/HDAC inhibitor-mediated lethality in MM cells.

Parallel studies were conducted to assess the effects of ROS generation on bortezomib/HDAC inhibitor-mediated perturbations in expression of various proteins implicated in the apoptotic process. As anticipated from the preceding findings, coadministration of L-NAC blocked bortezomib/NaB- and bortezomib/SAHA-induced PARP degradation in both U266 and MM.1S cells (Fig. 6*E*). Interestingly, L-NAC also largely prevented bortezomib/HDAC inhibitor-induced JNK activation and down-regulation of cyclin D1, XIAP, and Mcl-1 in both cell lines. In contrast, L-NAC failed to modify histone H3 and H4 acetylation in these cells. Together, these observations support the notion that ROS generation plays an important functional role in bortezomib/HDAC inhibitor-mediated mitochondrial injury, apoptosis, and perturbations in signaling pathways in MM cells.

Bortezomib/HDAC Inhibitor-Mediated Down-Regulation of Cyclin D1, XIAP, and Mcl-1 Is Caspase Dependent. To determine what role, if any, caspase activation might play in diminished expression of cyclin D1, XIAP, and Mcl-1 in bortezomib/HDAC inhibitor-treated myeloma cells, U266 and MM.1S cells were sequentially exposed to these agents in the presence or absence of the broad caspase inhibitor BOC-D-fmk. As shown in Fig. 7, *A* and *B*, BOC-D-fmk substantially reduced

bortezomib/NaB- and bortezomib/SAHA-mediated apoptosis in both cell lines ($P < 0.01$ in each case). BOC-D-fmk also blocked PARP degradation and either significantly attenuated or abrogated the observed reductions in cyclin D1, Mcl-1, and XIAP expression in bortezomib/HDAC inhibitor-treated myeloma cells (Fig. 7*C*). These findings suggest that down-regulation of such proteins in bortezomib/HDAC inhibitor-treated cells represents, at least in part, a caspase-dependent effect.

Exogenous IL-6 and IGF-I Fail to Protect Myeloma Cells from Bortezomib/HDAC-Mediated Lethality. The ability of growth factors such as IL-6 and IGF-I to protect MM cells from the lethal effects of various stimuli, including dexamethasone, is well known (34, 35). To determine whether these growth factors could block bortezomib/HDAC inhibitor-associated lethality, U266 and MM.1S cells were exposed to bortezomib and either NaB or SAHA in the presence or absence of IL-6 (100 ng/ml) or IGF-I (400 ng/ml), after which apoptosis was assessed. In contrast to dexamethasone-induced lethality, which was significantly attenuated by coadministration of IL-6 or IGF-I ($P < 0.05$ in U266; $P < 0.01$ in MM.1S), these growth factors failed to reduce bortezomib/NaB- or bortezomib/SAHA-mediated lethality in either of the myeloma cell lines ($P > 0.05$ in each case; Fig. 8, *A* and *B*). These findings indicate that in contrast to dexamethasone-induced lethality, bortezomib/HDAC inhibitor-mediated apoptosis operates through IL-6- and IGF-I-independent pathways.

Prior Exposure to Bortezomib Promotes HDAC Inhibitor-Mediated Lethality in Primary, Patient-Derived CD138$^+$ MM Cells. To determine whether these findings could be extended to primary, patient derived cells, CD138$^+$ MM cells were obtained from the bone marrows of two patients with MM and exposed to bortezomib ± NaB or SAHA as described for U266 and MM1.S cells, after which the extent of apoptosis was assessed. As shown in Fig. 9, CD138$^+$ cells from two separate patients exhibited relatively modest or no toxicity
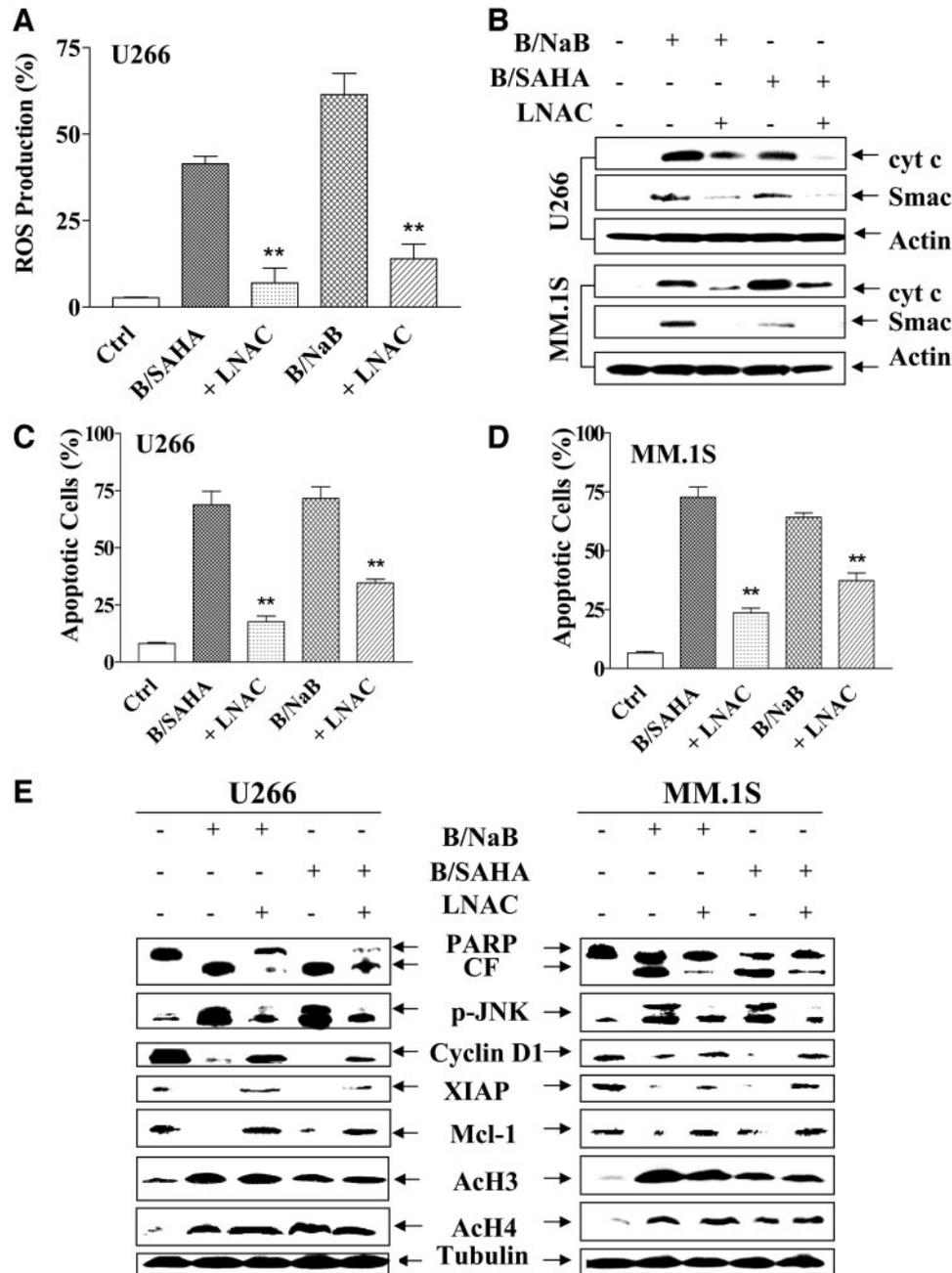
Fig. 6 Reactive oxygen species generation contributes to bortezomib/histone deacetylase inhibitor-mediated mitochondrial injury and apoptosis in multiple myeloma (MM) cells. After preincubation with 15 mM *N*-acetyl-L-cysteine for 3 h, U266 cells were treated with 1 μM suberoylanilide hydroxamic acid or 1 mM sodium butyrate for 6 h after a 6-h pretreatment with 2.4 nM bortezomib. At the end of this period, the percentage of cells displaying increased reactive oxygen species production was determined by monitoring dihydro-dichlorodihydroflurescein staining by flow cytometry as described in "Materials and Methods" (*A*). MM cells were sequentially treated with bortezomib (*top panels,* U266, 2.4 nM; *bottom panels,* MM.1S, 2.3 nM) for 6 h followed by 1 μM suberoylanilide hydroxamic acid or 1 mM sodium butyrate for 20 h, cytosolic (S-100) fractions were obtained as described in "Materials and Methods," and expression of cytochrome *c* and Smac/DIABLO was monitored by Western blot (*B*). U266 (*C*) and MM.1S cells (*D*) were treated as described in *B*, after which the percentage of cells exhibiting apoptotic morphology was determined by evaluating Wright Giemsa-stained cytospin preparations. Alternatively, the cells were lysed and subjected to Western blot analysis using the indicated primary antibodies (*E*). *CF,* cleavage fragment. For *A, C,* and *D,* results represent the means ± SD for three separate experiments performed in triplicate. ∗∗, significantly lower (*P* < 0.01) than values for cells treated with bortezomib → histone deacetylase inhibitors in the absence of *N*-acetyl-L-cysteine. For *B* and *E*, each lane was loaded with 30 μg of protein; the blots were stripped and reprobed with antiactin or antitubulin antibody to ensure equal loading and transfer. The results are representative of three separate experiments.
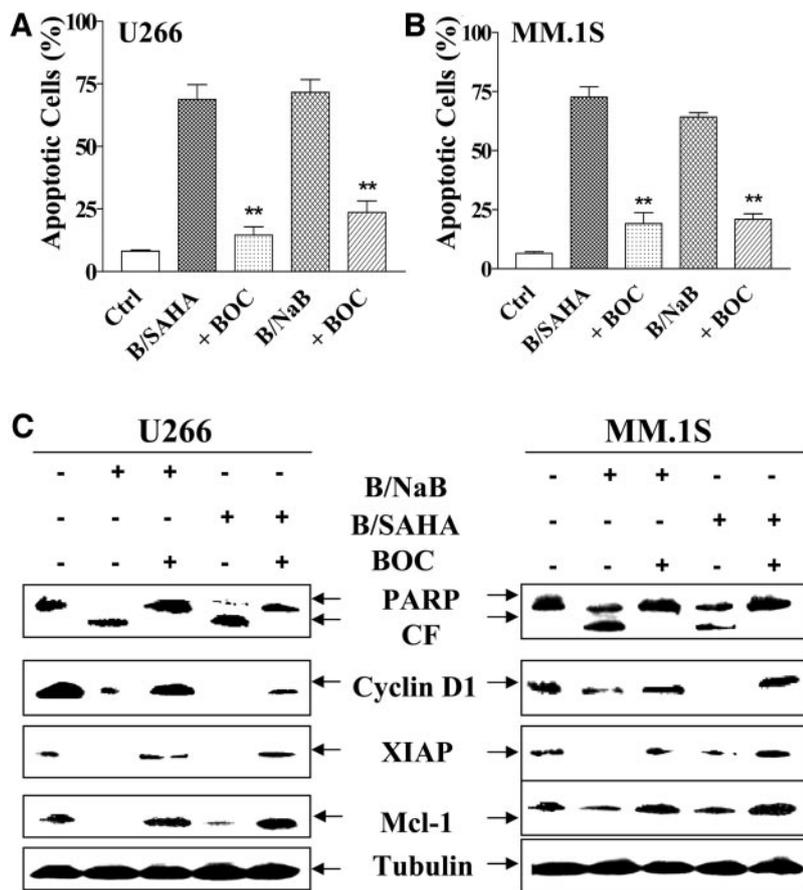
Fig. 7 The caspase inhibitor BOC-D-fmk attenuates bortezomib/histone deacetylase inhibitor-induced apoptosis and down-regulation of antiapoptotic molecules in multiple myeloma (MM) cells. MM cells were sequentially treated with bortezomib (*A,* U266, 2.4 nM; *B,* MM.1S, 2.3 nM) for 6 h followed by 1 μM suberoylanilide hydroxamic acid or 1 mM sodium butyrate for 20 h in either the absence or presence of 20 μM BOC-D-fmk, after which the percentage of cells exhibiting apoptotic morphology was determined by evaluating Wright Giemsa-stained cytospin preparations. Results represent the means ± SD for three separate experiments performed in triplicate. **, significantly lower than values for cells treated with bortezomib → histone deacetylase inhibitors in the absence of BOC-D-fmk ($P < 0.01$). Alternatively, cells were lysed and subjected to Western blot analysis using the indicated primary antibodies (*C*). *CF,* cleavage fragment. Each lane was loaded with 30 μg of protein; blots were stripped and reprobed with antitubulin antibody to ensure equal loading and transfer. Two additional studies yielded equivalent results.

after exposure to bortezomib or HDAC inhibitors administered individually. However, sequential exposure resulted in a very pronounced increase in apoptosis in these cells, analogous to results obtained with continuously cultured myeloma cell lines. Interestingly, the CD138⁻ bone marrow cell population was largely unaffected by exposure to bortezomib and HDAC inhibitors, alone or in combination. These findings indicate that sequential exposure to bortezomib and HDAC inhibitors leads to a marked increase in apoptosis in at least some primary patient-derived myeloma cells. They also raise the possibility that the selective lethality proteasome inhibitors exhibit toward neoplastic cells (36) may extend to combinations involving HDAC inhibitors.

DISCUSSION

The present results indicate that combined exposure of MM cells to the proteasome inhibitor bortezomib in conjunction with one of two clinically relevant HDAC inhibitors (*e.g.,* NaB or SAHA) results in a marked increase in mitochondrial injury, caspase activation, and the synergistic induction of apoptosis. Earlier studies suggested that combined exposure of Y79 neuroblastoma cells to butyrate and the proteasome inhibitor MG-132 induced a striking increase in cytochrome *c* release, culminating in cell death (23), and our group has made similar observations in Bcr/Abl⁺ myeloid leukemia cells exposed to

HDAC inhibitors in combination with bortezomib (24). The ability of proteasome inhibitors such as bortezomib to trigger apoptosis in MM cells *in vitro* (14) and the documented activity of bortezomib in patients with MM, including those with refractory disease (9, 15), have established a clear indication for this agent in patients with plasma cell dyscrasias. Very recently, several reports have shown that HDAC inhibitors, including SAHA (22) and the novel hydroxamic acid derivative LAQ824, are active against myeloma cells in culture (37), suggesting a possible role for such agents in the therapeutic armamentarium against this disease. Consequently, the finding that MM cells are particularly susceptible to a regimen in which proteasome and HDAC inhibitors are combined has potential therapeutic implications.

The mechanism by which HDAC inhibitors induce apoptosis in malignant cells is not known with certainty, but there is evidence that this process may involve Bid cleavage and generation of ROS (18) and, most recently, acetylation of nonhistone proteins (*e.g.,* Hsp90), resulting in interruption of survival signal transduction pathways (38). In leukemia cells, HDAC inhibitors such as SAHA induce maturation at relatively low concentrations (39), whereas apoptosis ensues in association with mitochondrial injury and caspase activation when HDAC inhibitors are administered at higher concentrations (40). In this context, SAHA has recently been shown to induce apoptosis in myeloma cells (*e.g.,* MM.1S)

Fig. 8 Bortezomib and histone deacety-lase inhibitors induce cell death in multiple myeloma (MM) cells in an interleukin (IL)-6- and insulin-like growth factor-independent manner. MM cells were incubated for 20 h with 1 μM suberoylanilide hydroxamic acid or 1 mM sodium butyrate after a 6-h pretreatment with bortezomib (*A,* U266, 2.4 nM; *B,* MM.1S, 2.3 nM) in either the presence or absence of 100 ng/ml IL-6 (*left graphs*) or 400 ng/ml insulin-like growth factor I (*right graphs*). At the end of this period, the percentage of cells exhibiting apoptotic morphology was determined by evaluating Wright Giemsa-stained cytospin preparations. Results represent the means ± SD for three separate experiments performed in triplicate. For comparison, cells were exposed to 100 μM dexamethasone for 24 h in the presence or absence of IL-6 or insulin-like growth factor I. *Asterisk* indicates values significantly less than the values for dexamethasone-treated cells in the absence of IL-6 or IGF-I (∗, $P < 0.05$; ∗∗, $P < 0.01$).
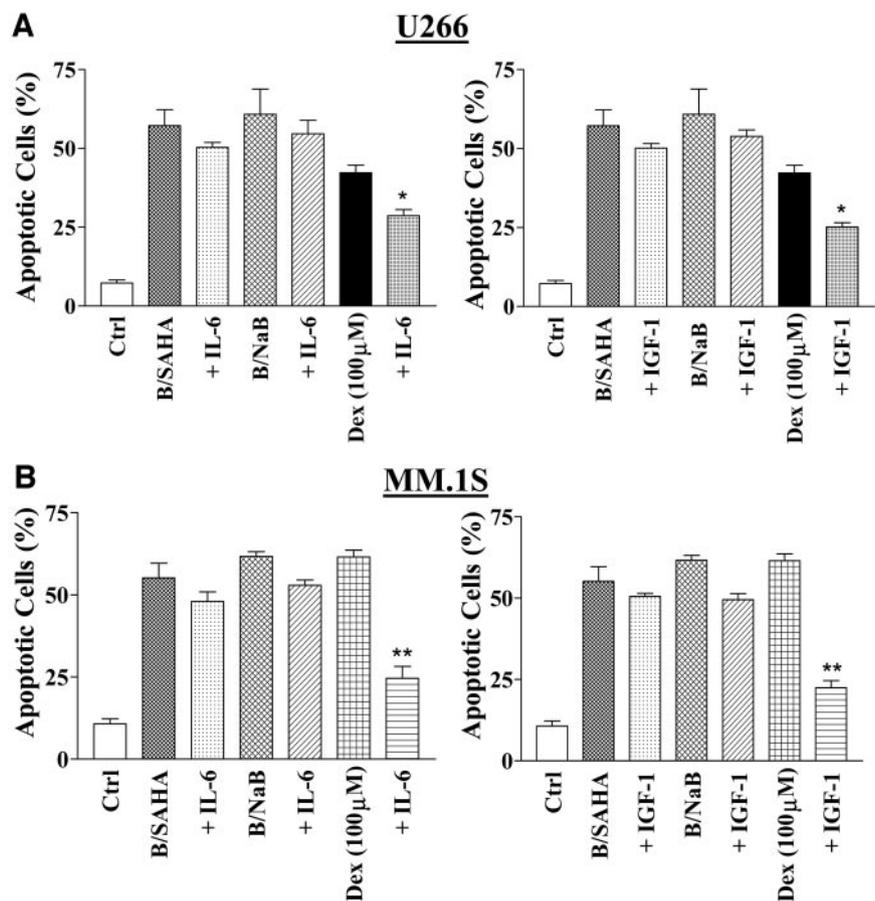
through a process that does not involve activation of caspase 3, 9, and 8 (22). In accord with these findings, SAHA, when administered alone at relatively nontoxic concentrations, also failed to trigger caspase activation or mitochondrial injury. However, coadministration of bortezomib with HDAC inhibitors resulted in activation of these caspases, as well as release of the proapoptotic proteins cytochrome *c* and Smac/DIABLO into the cytosolic S-100 fraction. These events suggest that bortezomib lowers the threshold for HDAC inhibitor-mediated mitochondrial injury and subsequent activation of the caspase cascade. It is noteworthy that results of an earlier study suggested that in MM cells, different stimuli (*e.g.,* dexamethasone *versus* ionizing radiation) may elicit a distinct pattern of mitochondrial injury [*e.g.,* cytochrome *c versus* Smac/DIABLO release (41)]. The ability of the bortezomib/HDAC inhibitor combination to induce release of both proteins suggests that this regimen activates a common pathway of mitochondrial injury.

The NF-κB pathway is known to play a critical role in myeloma cell survival (6), and the capacity of bortezomib to interrupt NF-κB signaling is thought to play a key role in the activity of this agent against myeloma cells (11). Consistent with these findings, bortezomib, when administered at a low concentration, modestly reduced NF-κB DNA binding in U266 cells. HDAC inhibitors have been shown to exert pleiotropic effects on NF-κB activity in various cell types, including increases in activity in some cells (42) and reductions in others

(43). In a recent study, LAQ824, particularly when administered at a toxic concentration, reduced NF-κB activity in myeloma cells (37). However, in the present study, exposure of cells to SAHA or NaB at relatively low, nonlethal concentrations resulted in an increase in activity. Whether this discrepancy reflects concentration-, drug-, or cell type-specific differences remains to be determined. In any case, combined exposure of U266 cells to bortezomib and HDAC inhibitors was associated with a very substantial decline in NF-κB activity. Given the dependence of myeloma cells on NF-κB activation for continued survival (6), the possibility that this effect contributes to the lethal actions of the bortezomib/HDAC inhibitor regimen seems plausible. It may also be relevant that recent studies from our laboratory suggest that disruption of the NF-κB cascade (*e.g.,* by molecular or pharmacological strategies) sensitizes myeloid leukemia cells to the lethal actions of HDAC inhibitors (44).

Combined exposure of myeloma cells to bortezomib and HDAC inhibitors was associated with several perturbations in signaling and cell cycle-regulatory proteins that might also play a role in the lethal effects of this combination. For example, combined exposure of myeloma cells to bortezomib/HDAC inhibitors induced activation of the stress-related kinase JNK, which has been associated with promotion of mitochondrial injury and apoptosis (45, 46). More recently, JNK activation has been implicated in induction of myeloma cell death by bort-
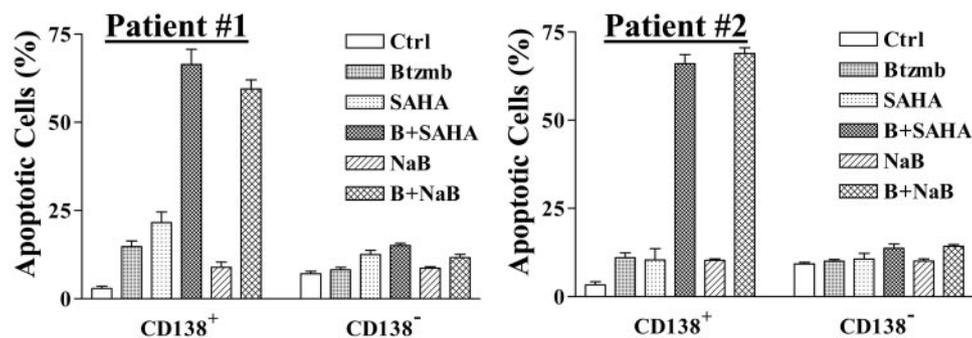
Fig. 9 Bortezomib/histone deacetylase inhibitor regimen selectively exerts lethality toward CD138$^+$ cells obtained from multiple myeloma patients. CD138$^+$ and CD138$^-$ cells were isolated from the bone marrow of two multiple myeloma patients as described in "Materials and Methods" and sequentially treated with 3 nM bortezomib (6 h) followed by 1.5 μM suberoylanilide hydroxamic acid or 1 mM sodium butyrate (24 h), respectively. At the end of this period, the percentage of cells exhibiting apoptotic morphology was determined by evaluating Wright Giemsa-stained cytospin preparations. Results represent the means ± SD for the experiments in triplicate.

ezomib (14). Consistent with previous reports (24), SAHA and NaB induced p21^{CIP1} in myeloma cells, although total levels of this protein did not change substantially with the addition of bortezomib. However, a p21^{CIP1} cleavage product, which has been shown to exert proapoptotic actions (47), was noted in cells exposed to both agents. Similarly, a Bcl-2 cleavage product, which has also been linked to cell death (32), was also observed in cells treated with bortezomib and HDAC inhibitors. Although these presumably represent secondary, caspase-dependent events, it is conceivable that they may contribute to the apoptotic process by promoting activation of the caspase cascade.

Combined treatment with bortezomib and HDAC inhibitors also led to down-regulation of Mcl-1, XIAP, and cyclin D1. Of these, Mcl-1 is thought to play a particularly important role in myeloma cell survival (48). However, the ability of the caspase inhibitor BOC-D-fmk to block down-regulation of these proteins indicates that diminished expression represents a secondary rather than a primary event in induction of cell death. Nevertheless, reductions in levels of these proteins may serve to amplify the apoptotic process by enhancing mitochondrial injury, promoting caspase activation, and/or by triggering cell cycle perturbations that lower the cell death threshold.

The present results provide further support for the notion that disruption of cellular redox state may represent an important mechanism underlying myeloma cell death after exposure to novel agents, alone and in combination. For example, the susceptibility of myeloma cells to arsenic trioxide has been attributed to free radical-mediated injury (49). In addition, there is accumulating evidence that proteasome inhibitors may act through a similar mechanism. For example, the lethal effects of relatively high concentrations of bortezomib (*e.g.,* 100 nM) in lung cancer cells have recently been shown to proceed through a ROS-dependent mechanism (33), as has induction of apoptosis in Bcr/Abl$^+$ myeloid leukemia cells by the combination of bortezomib and HDAC inhibitors (24). Notably, the lethality of HDAC inhibitors in various neoplastic cells, including those of hematopoietic origin, has also been related to free radical-mediated injury (17, 19). The ability of the antioxidant L-NAC to attenuate both bortezomib/HDAC inhibitor-mediated ROS generation and lethality supports a role for free radical generation in the activity of this regimen. Interestingly, L-NAC also attenuated bortezomib/HDAC inhibitor-mediated down-regulation

of Mcl-1, XIAP, and cyclin D1, presumably by preventing mitochondrial injury and activation of the caspase cascade. L-NAC also blocked phosphorylation/activation of JNK, a phenomenon known to play an important role in mediating the cellular response to oxidative injury (50). Finally, activation of NF-κB represents a major component the cellular defense mechanism to oxidative stress (51). Thus, the bortezomib/HDAC inhibitor regimen may trigger cell death through multiple interacting mechanisms, including increasing ROS generation and disabling of the cytoprotective NF-κB pathway.

It is important to note that the bortezomib/HDAC inhibitor regimen displayed substantial toxicity toward primary, patient-derived CD138$^+$ cells and that it was relatively sparing toward their CD138$^-$ counterparts. The basis for the selective toxicity of bortezomib and other proteasome inhibitors toward neoplastic cells (36) is not known with certainty, but in the case of MM, may stem from the dependence of myeloma cells on an intact NF-κB pathway for survival (6). Whatever the mechanism, it is conceivable that the factor or factors that contribute to the favorable therapeutic index of bortezomib in MM (11) may be extended to the bortezomib/HDAC inhibitor regimen. Given the documented activity of bortezomib in MM (9, 15), promising preclinical evidence suggesting a role for HDAC inhibitors in this disease (22, 37), and evidence of synergistic interactions between these agents in cultured myeloma cells and primary specimens, further exploration of this strategy in MM appears warranted. Accordingly, such efforts are currently in progress.

REFERENCES

1. Diagnosis and management of multiple myeloma: UK myeloma forum. British Committee for Standards in Haematology. Br J Haematol 2001;115:522–40.

2. Lauta VM. A review of the cytokine network in multiple myeloma: diagnostic, prognostic, and therapeutic implications. Cancer (Phila) 2003;97:2440–52.

3. Ferlin M, Noraz N, Hertogh C, et al. Insulin-like growth factor induces the survival and proliferation of myeloma cells through an interleukin-6-independent transduction pathway. Br J Haematol 2000; 111:626–34.

4. Croonquist PA, Linden MA, Zhao F, Van Ness BG. Gene profiling of a myeloma cell line reveals similarities and unique signatures among

IL-6 response, N-ras-activating mutations, and coculture with bone marrow stromal cells. Blood 2003;102:2581–92.

5. Hsu J, Shi Y, Krajewski S, et al. The AKT kinase is activated in multiple myeloma tumor cells. Blood 2001;98:2853–5.

6. Berenson JR, Ma HM, Vescio R. The role of nuclear factor-kappaB in the biology and treatment of multiple myeloma. Semin Oncol 2001; 28:626–33.

7. Mileshkin L, Biagi JJ, Mitchell P, et al. Multicenter Phase 2 trial of thalidomide in relapsed/refractory multiple myeloma: adverse prognostic impact of advanced age. Blood 2003;102:69–77.

8. Munshi NC, Tricot G, Desikan R, et al. Clinical activity of arsenic trioxide for the treatment of multiple myeloma. Leukemia (Baltimore) 2002;16:1835–72.

9. Richardson PG, Barlogie B, Berenson J, et al. Phase 2 study of bortezomib in relapsed, refractory myeloma. N Engl J Med 2003;348:2609–17.

10. Adams J. The proteasome: structure, function, and role in the cell. Cancer Treat Rev 2003;29(Suppl 1):3–9.

11. Mitsiades N, Mitsiades CS, Poulaki V, et al. Biologic sequelae of nuclear factor-kappaB blockade in multiple myeloma: therapeutic applications. Blood 2002;99:4079–86.

12. Ling YH, Liebes L, Jiang JD, et al. Mechanisms of proteasome inhibitor PS-341-induced G_2-M-phase arrest and apoptosis in human non-small cell lung cancer cell lines. Clin Cancer Res 2003;9:1145–54.

13. Orlowski RZ, Stinchcombe TE, Mitchell BS, et al. Phase I trial of the proteasome inhibitor PS-341 in patients with refractory hematologic malignancies J Clin Oncol 2002;20:4420–7.

14. Hideshima T, Mitsiades C, Akiyama M, et al. Molecular mechanisms mediating antimyeloma activity of proteasome inhibitor PS-341. Blood 2003;101:1530–4.

15. Richardson P. Clinical update: proteasome inhibitors in hematologic malignancies. Cancer Treat Rev 2003;29(Suppl 1):33–9.

16. Nakatani Y. Histone acetylases: versatile players. Genes Cells 2001;6:79–86.

17. Johnstone RW. Histone-deacetylase inhibitors: novel drugs for the treatment of cancer. Nat Rev Drug Discov 2002;1:287–99.

18. Ruefli AA, Ausserlechner MJ, Bernhard D, et al. The histone deacetylase inhibitor and chemotherapeutic agent suberoylanilide hydroxamic acid (SAHA) induces a cell-death pathway characterized by cleavage of Bid and production of reactive oxygen species. Proc Natl Acad Sci USA 2001;98:10833–8.

19. Rosato RR, Almenara JA, Grant S. The histone deacetylase inhibitor MS-275 promotes differentiation or apoptosis in human leukemia cells through a process regulated by generation of reactive oxygen species and induction of p21CIP1/WAF1 1. Cancer Res 2003;63:3637–45.

20. Rosato RR, Grant S. Histone deacetylase inhibitors in cancer therapy. Cancer Biol Ther 2003;2:30–7.

21. Marks P, Rifkind RA, Richon VM, et al. Histone deacetylases and cancer: causes and therapies. Nat Rev Cancer 2001;1:194–202.

22. Mitsiades N, Mitsiades CS, Richardson PG, et al. Molecular sequelae of histone deacetylase inhibition in human malignant B cells. Blood 2003;101:4055–62.

23. Giuliano M, Lauricella M, Calvaruso G, et al. The apoptotic effects and synergistic interaction of sodium butyrate and MG132 in human retinoblastoma Y79 cells. Cancer Res 1999;59:5586–95.

24. Yu C, Rahmani M, Conrad D, et al. The proteasome inhibitor bortezomib interacts synergistically with histone deacetylase inhibitors to induce apoptosis in Bcr/Abl+ cells sensitive and resistant to STI571. Blood 2003;102:3765–74.

25. Moalli PA, Pillay S, Weiner D, Leikin R, Rosen ST. A mechanism of resistance to glucocorticoids in multiple myeloma: transient expression of a truncated glucocorticoid receptor mRNA. Blood 1992;79:213–22.

26. Dalton WS, Durie BG, Alberts DS, Gerlach JH, Cress AE. Characterization of a new drug-resistant human myeloma cell line that expresses P-glycoprotein. Cancer Res 1986;46:5125–30.

27. Dai Y, Landowski TH, Rosen ST, Dent P, Grant S. Combined treatment with the checkpoint abrogator UCN-01 and MEK1/2 inhibitors potently induces apoptosis in drug-sensitive and -resistant myeloma cells through an IL-6-independent mechanism. Blood 2002;100:3333–43.

28. Dai Y, Yu C, Singh V, et al. Pharmacological inhibitors of the mitogen-activated protein kinase (MAPK) kinase/MAPK cascade interact synergistically with UCN-01 to induce mitochondrial dysfunction and apoptosis in human leukemia cells. Cancer Res 2001;61:5106–15.

29. Leach JK, Tuyle GV, Lin PS, Schmidt-Ullrich R, Mikkelsen RB. Ionizing radiation-induced, mitochondria-dependent generation of reactive oxygen/nitrogen. Cancer Res 2001;61:3894–901.

30. Dai Y, Rahmani M, Grant S. Proteasome inhibitors potentiate leukemic cell apoptosis induced by the cyclin-dependent kinase inhibitor flavopiridol through a SAPK/JNK- and NF-kappaB-dependent process. Oncogene 2003;22:7108–22.

31. Chou TC, Talalay P. Quantitative analysis of dose-effect relationships: the combined effects of multiple drugs or enzyme inhibitors. Adv Enzyme Regul 1984;22:27–55.

32. Liang Y, Nylander KD, Yan C, Schor NF. Role of caspase 3-dependent Bcl-2 cleavage in potentiation of apoptosis by Bcl-2. Mol Pharmacol 2002;61:142–9.

33. Ling YH, Liebes L, Zou Y, Perez-Soler R. Reactive oxygen species generation and mitochondrial dysfunction in the apoptotic response to bortezomib, a novel proteasome inhibitor, in human H460 non-small cell lung cancer cells. J Biol Chem 2003;278:33714–23.

34. Tassone P, Galea E, Forciniti S, Tagliaferri P, Venuta S. The IL-6 receptor super-antagonist Sant7 enhances antiproliferative and apoptotic effects induced by dexamethasone and zoledronic acid on multiple myeloma cells. Int J Oncol 2002;21:867–73.

35. Ogawa M, Nishiura T, Oritani K, et al. Cytokines prevent dexamethasone-induced apoptosis via the activation of mitogen-activated protein kinase and phosphatidylinositol 3-kinase pathways in a new multiple myeloma cell line. Cancer Res 2000;60:4262–9.

36. Ma MH, Yang HH, Parker K, et al. The proteasome inhibitor PS-341 markedly enhances sensitivity of multiple myeloma tumor cells to chemotherapeutic agents. Clin Cancer Res 2003;9:1136–44.

37. Catley L, Weisberg E, Tai YT, et al. NVP-LAQ824 is a potent novel histone deacetylase inhibitor with significant activity against multiple myeloma Blood 2003;102:2615–22.

38. Nimmanapalli R, Fuino L, Bali P, et al. Histone deacetylase inhibitor LAQ824 both lowers expression and promotes proteasomal degradation of Bcr-Abl and induces apoptosis of imatinib mesylate-sensitive or -refractory chronic myelogenous leukemia-blast crisis cells. Cancer Res 2003;63:5126–35.

39. Almenara J, Rosato R, Grant S. Synergistic induction of mitochondrial damage and apoptosis in human leukemia cells by flavopiridol and the histone deacetylase inhibitor suberoylanilide hydroxamic acid (SAHA). Leukemia (Baltimore) 2002;16:1331–43.

40. Vrana JA, Decker RH, Johnson CR, et al. Induction of apoptosis in U937 human leukemia cells by suberoylanilide hydroxamic acid (SAHA) proceeds through pathways that are regulated by Bcl-2/Bcl-XL, c-Jun, and p21CIP1, but independent of p53. Oncogene 1999;18:7016–25.

41. Chauhan D, Hideshima T, Rosen S, et al. Apaf-1/cytochrome c-independent and Smac-dependent induction of apoptosis in multiple myeloma (MM) cells. J Biol Chem 2001;276:24453–6.

42. Suzuki M, Shinohara F, Sato K, et al. Interleukin-1beta converting enzyme subfamily inhibitors prevent induction of CD86 molecules by butyrate through a CREB-dependent mechanism in HL60 cells. Immunology 2003;108:375–83.

43. Yin L, Laevsky G, Giardina C. Butyrate suppression of colonocyte NF-kappa B activation and cellular proteasome activity. J Biol Chem 2001;276:44641–6.

44. Dai Y, Rahmani M, Grant S. An intact NF-kappaB pathway is required for histone deacetylase inhibitor-induced G_1 arrest and maturation in U937 human myeloid leukemia cells. Cell Cycle 2003;2:467–72.

45. Xia Z, Dickens M, Raingeaud J, Davis RJ, Greenberg ME. Opposing effects of ERK and JNK-p38 MAP kinases on apoptosis. Science (Wash DC) 1995;270:1326–31.

46. Chauhan D, Li G, Hideshima T, et al. JNK-dependent release of mitochondrial protein, Smac, during apoptosis in multiple myeloma (MM) cells. J Biol Chem 2003;278:17593–6.

47. Xiang H, Fox JA, Totpal K, et al. Enhanced tumor killing by Apo2L/TRAIL and CPT-11 co-treatment is associated with p21 cleavage and differential regulation of Apo2L/TRAIL ligand and its receptors. Oncogene 2002;21:3611–9.

48. Jourdan M, Veyrune JL, Vos JD, et al. A major role for Mcl-1 antiapoptotic protein in the IL-6-induced survival of human myeloma cells. Oncogene 2003;22:2950–9.

49. Grad JM, Bahlis NJ, Reis I, et al. Ascorbic acid enhances arsenic trioxide-induced cytotoxicity in multiple myeloma cells. Blood 2001; 98:805–13.

50. Li Y, Arita Y, Koo HC, Davis JM, Kazzaz JA. Inhibition of JNK pathway improves cell viability in response to oxidant injury. Am J Respir Cell Mol Biol 2003; 779–83.

51. Tanaka H, Matsumura I, Ezoe S, et al. 2F1 and c-Myc potentiate apoptosis through inhibition of NF-kappaB activity that facilitates Mn-SOD-mediated ROS elimination. Mol Cell 2002;9:1017–29.